Proceedings of the 17th International Heat Transfer Conference, IHTC-17
August 14-18, 2023, Cape Town, South Africa

IHTC17

ASSESSMENT OF A SPECTRAL VANISHING VISCOSITY LES MODEL FOR 3D RAYLEIGH-BÉNARD CONVECTION IN A CUBIC CELL

M. Delort-Laval,[1,2] L. Soucasse,[1,*] Ph. Rivière,[1] A. Soufiani[1]

[1]Laboratoire EM2C, CNRS, CentraleSupélec, Université Paris-Saclay, 8-10 rue Joliot Curie, 91192 Gif-sur-Yvette, France
[2]ADEME, 155 bis Avenue Pierre Brossolette, 92240 Montrouge , France

ABSTRACT

Rayleigh-Bénard (RB) convection is a challenging topic for both academic research and for several applications in the field of atmospheric physics, industrial applications, and building insulation. The actual applications involve high Rayleigh or Grashoff numbers but the Direct Numerical Simulations (DNS) remain limited to relatively small values of these numbers. Approximate models are required for the prediction of flow fields and heat transfer at higher numbers. The aim of this study is to assess the ability of a Large Eddy Simulation (LES) model to predict accurate mean values and second order moments of temperature and velocity fields. The reference fields are provided by DNS simulations under the Boussinesq approximation in a RB cell filled with air at a Rayleigh number (Ra) up to 10^9. The employed numerical DNS method is based on a Tchebychev pseudo-spectral method and the most appropriate LES model in this case appears to be the Spectral Vanishing Viscosity (SVV) model where high order modes are exponentially damped to stabilize the numerical scheme. The predicted mean velocity and temperature fields from this LES model, as well as their second order moments, are compared to DNS values. A sensitivity study to the SVV parameters, i.e. the Tchebychev mode cutoff and the damping amplitude, is carried out. The model appears to be a promising approach for accurate predictions at much higher Rayleigh numbers.

KEY WORDS: Rayleigh-Bénard convection, Spectral Vanishing Viscosity, heat transfer, unsteady flow regimes, 3D cubical cavity.

1. INTRODUCTION

Large Eddy Simulation (LES) consists in resolving the large scales of a fluid flow and modelling the effects of the small scales, mainly the dissipation of the energy. Many models have been proposed since the pioneering study of Smagorinsky [9]. However, these models are not well suited for spectral numerical methods and a different approach has been proposed by Tadmor in 1989, the Spectral Vanishing Viscosity (SVV) model [5, 10]. Spectral methods have the particularity of bringing very few numerical dissipation to the solution, wich gives them a very high-order accuracy. However, if not enough modes are used in the spectral representation of the solution, the energy that is transferred to the high modes is not dissipated along the way. The lack of dissipation due to the coarse representation is not compensated by the numerical dissipation and the numerical scheme is unstable.

To avoid that, Tadmor introduced a new term in the equation designed to add a dissipative component, in order to stabilize the spectral methods. It appears as an operator acting like an hyperviscosity affecting only the high

*Corresponding L. Soucasse: laurent.soucasse@centralesupelec.fr

modes of the spectral representation, dealing with the energy transfer to these modes. The ideal form of the operator was discussed in [1] and took its exponential form with the work of [4] and [7], which has been widely used since then [6, 8].

The SVV operator depends on two main parameters : a cut-off mode M and a weight ϵ. The influence of these two parameters and their ideal values were the subject of many studies, both theoretical and numerical, since the beginning of the SVV approach [1, 4–7, 10]. We propose here a parametric study in which we analyse the results obtained with several configurations, in order to evaluate the influence of these parameters on both the stability of the simulation and the accuracy of the results. Results with the SVV model are compared to results obtained via Direct Numerical Simulation (DNS) obtained in a previous study [2].

2. STUDIED CONFIGURATION

We consider a cubical cavity, heated from the bottom and cooled from the top walls, both being considered isothermal ; the lateral walls are assumed adiabatic (figure 1). The cavity is filled with transparent air at a mean temperature of $T_0 = 300K$ and at atmospheric pressure ($\mathrm{Pr} = 0.707$). This system is governed by the Navier-Stokes equations under the Boussinesq approximation. The solutions of the system only depend on two parameters the Rayleigh (Ra) and Prandtl (Pr) numbers, defined by:

$$\mathrm{Ra} = \frac{g\beta\Delta T L^3}{\nu a} \quad ; \quad \mathrm{Pr} = \frac{\nu}{a} \tag{1}$$

with g is the gravitational acceleration, $\beta = 1/T_0$ is the thermal expansion coefficient, $\Delta T = T_{\mathrm{hot}} - T_{\mathrm{cold}}$ is the temperature difference between the isothermal walls, ν is the kinematic viscosity and a is the thermal diffusivity.

The system of equations is solved using a Chebychev spectral method for the Navier-Stokes equations and parallelisation of the code is ensured via domain decomposition along the vertical axis. More details on the method can be found in [2, 11, 12].

The reference velocity and time are chosen according to the work of Patterson and Imberger [3], and the dimensionless temperature θ is defined as follows :

$$u_{ref} = \frac{a\sqrt{\mathrm{Ra}}}{L} \quad ; \quad t_{ref} = \frac{L^2}{a\sqrt{\mathrm{Ra}}} \quad ; \quad \theta = \frac{T - T_0}{\Delta T} \tag{2}$$

These settings allow the dimensionless velocity $\boldsymbol{u}$ to remain at the same order of magnitude from $\mathrm{Ra} = 10^6$ and higher [2].

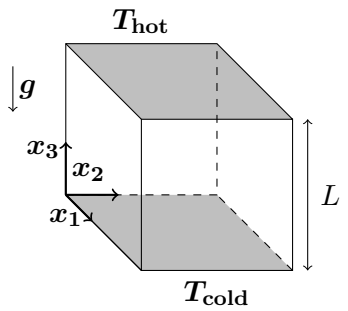

Fig. 1 The cubical Rayleigh-Bénard cavity with isothermal top and bottom walls and adiabatic lateral walls.

3. GOVERNING EQUATIONS AND THE SPECTRAL VANISHING VISCOSITY MODEL

The nondimensional mass, momentum and energy balance equations, with the SVV model, are given by equations (3,4,5).

$$\boldsymbol{\nabla} \cdot \boldsymbol{u} = 0 \tag{3}$$

$$\frac{\partial \boldsymbol{u}}{\partial t} + \boldsymbol{u} \cdot \boldsymbol{\nabla} \boldsymbol{u} = -\boldsymbol{\nabla} p + \mathrm{Pr}\theta \boldsymbol{e_z} + \frac{\mathrm{Pr}}{\sqrt{\mathrm{Ra}}} \boldsymbol{\nabla}^2 \boldsymbol{u} + \boldsymbol{\nabla} \cdot \left(\epsilon \tilde{\boldsymbol{\nabla}} \boldsymbol{u} \right) \tag{4}$$

$$\frac{\partial \theta}{\partial t} + \boldsymbol{u} \cdot \boldsymbol{\nabla} \theta = \frac{1}{\sqrt{\mathrm{Ra}}} \boldsymbol{\nabla}^2 \theta + \boldsymbol{\nabla} \cdot \left(\epsilon \tilde{\boldsymbol{\nabla}} \theta \right) \tag{5}$$

In the momentum and energy equations, the SVV term is added, $\boldsymbol{\nabla} \cdot \left(\epsilon \tilde{\boldsymbol{\nabla}} \right)$, with $\tilde{\boldsymbol{\nabla}} = Q \boldsymbol{\nabla}$ being the gradient operator $\boldsymbol{\nabla}$ modified by the SVV operator Q acting on its high-order modes, and ϵ the weight of the SVV model. The operator Q can be represented on a truncated Chebychev basis $(T_k)_{0 \leq k \leq N}$ as :

$$Q = \sum_{k=0}^{N} \widehat{Q_k} T_k, \tag{6}$$

and the spectral components of the decomposition are defined as

$$\widehat{Q_k} = \begin{cases} 0 & \text{if } k \leq M \\ \exp\left(-\frac{(k-N)^2}{(k-M)^2} \right) & \text{if } k > M \end{cases}. \tag{7}$$

M is the cut-off mode, from which the operator Q starts to act, with an exponential evolution. The SVV model acts therefore as an additionnal dissipation but only for the high modes of the spectral representation, that contain the excess of energy that has to be taken care of.

4. SENSITIVITY STUDY OF THE SVV MODEL TO THE PARAMETERS

4.1 Methodology

This parametric study consists in testing several values for the cut-off mode and the weight, for multiple coarsening of the mesh, and at two Rayleigh numbers. For each Rayleigh number, the reference for the number of modes is the one used in the DNS simulation : $N_{\mathrm{DNS}} = 160$ at $\mathrm{Ra} = 10^8$ and $N_{\mathrm{DNS}} = 320$ at $\mathrm{Ra} = 10^9$, along each direction of space. The number of modes used for the SVV simulations, N, is characterised by a Mesh Reduction Factor (MRF) according to $N = N_{\mathrm{DNS}}/\mathrm{MRF}$. Three MRF's are studied at $\mathrm{Ra} = 10^9$ and two at $\mathrm{Ra} = 10^8$. These are summarized in Table 1.

MRF	1 (DNS)	2	2.67	4
$\mathrm{Ra} = 10^8$	160 (8) [1200]	80 (4) [1200]	60 (3) [1200]	-
$\mathrm{Ra} = 10^9$	320 (16) [400]	160 (8) [400]	120 (6) [400]	80 (4) [400]

Table 1 Number of collocation points N in each direction, for each Rayleigh number and each MRF studied. In parenthesis, the number of domains in the vertical decomposition of the cavity (20 collocation points per domain, in the vertical direction). In brackets, the integration time interval for each simulation.

The weight ϵ is usually taken inversely proportional to the number of modes used in the spectral decomposition

M \ ϵ	$1/N$	$1/2N$	$1/3N$	$1/4N$
$N/2$	$N/2++$	$N/2+$	$N/2-$	$N/2--$
$2N/3$	$2N/3++$	$2N/3+$	$2N/3-$	$2N/3--$
$3N/4$	$3N/4++$	$3N/4+$	$3N/4-$	$3N/4--$
$4N/5$	$4N/5++$	$4N/5+$	$4N/5-$	$4N/5--$

Table 2 Parameters considered for the sensitivity study of the SVV model. In light gray, the configurations investigated in the study and their designations.

[1, 4, 6, 7, 10]. The following weights have been considered :

$$\epsilon \in \left\{ \frac{1}{N}, \frac{1}{2N}, \frac{1}{3N}, \frac{1}{4N} \right\}. \tag{8}$$

As for the cut-off mode, the stability of the SVV models in onedimensional simulations requires $M \simeq N^{\beta}$, with $\beta \leq 1/2$ [1] or even $\beta < 1/4$ [5, 10]. But in multidimensional simulations, the condition is not as strict and M is often taken as a fraction of N [1, 4, 7]. The following cut-off modes have thus been considered :

$$M \in \left\{ \frac{N}{2}, \frac{2N}{3}, \frac{3N}{4}, \frac{4N}{5} \right\}. \tag{9}$$

Table 2 summarizes all the 16 combinations of weight and cut-off mode that have to be studied, for the 3 MRF's at $\mathrm{Ra} = 10^9$ and two at $\mathrm{Ra} = 10^8$. To reduce the number of simulations, only half of these combinations were studied : the ones from the diagonal and the anti-diagonal of the table. The spectral representation of the corresponding operator $\epsilon\widehat{Q_k}$ is shown in figure 2 (a).

4.2 Sensitivity of SVV model to the parameters

The combinations of weight and cut-off mode were compared along two criteria: the ability to stabilize the simulation and the ability to accurately predict the basic fluxes in the cavity. Deeper investigations on the accuracy of SVV modelisation will concentrate on one model and are found in section 5.

4.2.1 Stability of the simulations Figure 2 presents, at $\mathrm{Ra} = 10^9$, the stability of the models for different MRF's. As the mesh gets coarser, it appears that the key element of the stability is the cut-off mode M, and the weight ϵ plays almost no role in it. The cut-off mode $M = 4N/5$ seems to be nearly ineffective for stabilizing the simulation: even for MRF = 2, the simulation is not stable for $\epsilon = 1/N$. As the MRF increases, more and more models are unstable and, for MRF = 4, only the models with $M = N/2$ are able to stabilize the simulation. The cut-off mode must therefore be the lowest possible to ensure the stability.

The simulations at $\mathrm{Ra} = 10^8$ were all stable, regardless of the parameters and MRF's studied. This can be explained by the lower level of turbulence than at $\mathrm{Ra} = 10^9$, conducting to a smaller amount of kinetic energy that needs to be dissipated at the high-order modes.

4.2.2 Prediction of the basic fluxes Tables 3 and 4 show, for all the models, Rayleigh numbers and studied MRF's, the conductive flux at the horizontal walls and the convective flux at the middle plane of the cavity, averaged over time and horizontal plane. Both at $\mathrm{Ra} = 10^8$ and $\mathrm{Ra} = 10^9$, the accuracy of the results decreases as the MRF increases, for every model. For MRF = 2, the SVV model is able to predict accurately both the Nusselt number at the wall and the convective flux in the middle. The accuracy of the model decreases for the lower values of the cut-off mode: this is specially true for $M = N/2$, which gives notably significant differences with the values obtained via DNS.

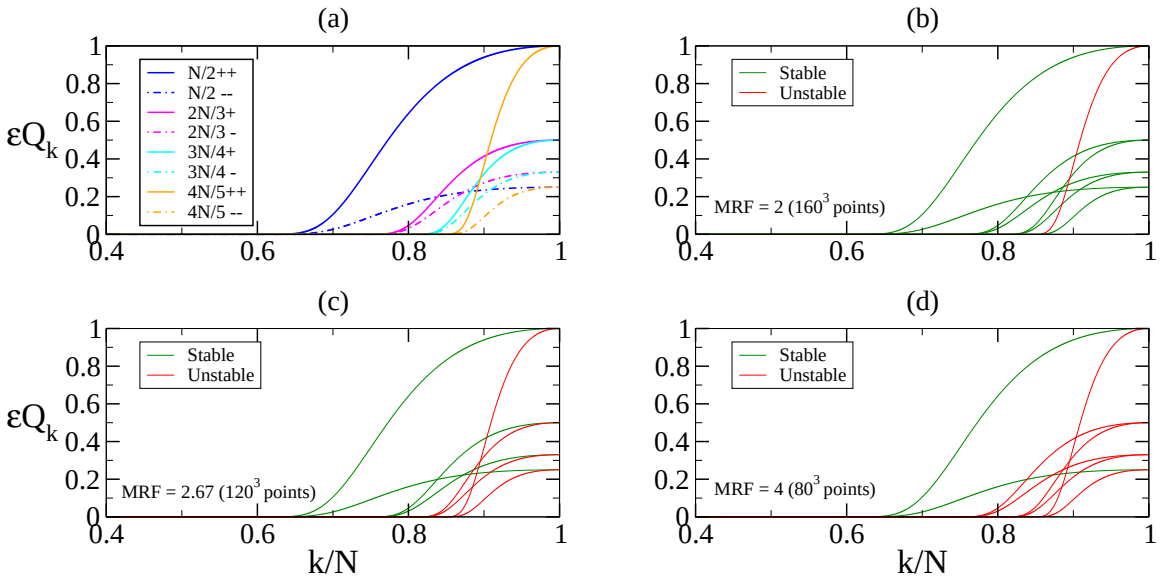

Fig. 2 Spectral representation of the studied SVV parameter configurations (a) and the numerical stability for different Mesh Reduction Factors (MRF= N_{DNS}/N) (b), (c) (d). $\mathrm{Ra} = 10^9$.

Here again, the weight seems to have a secondary role compared to the cut-off mode. A high enough cut-off mode ensures good prediction of these basic fluxes, regardless of the weight. It is only when the cut-off mode is too low to guarantee a good accuracy that the weight can play a minor role in correcting the error.

Ra	10^8				10^9					
MRF (Mesh) / Case	2.67 (60)		2 (80)		4 (80)		2.67 (120)		2 (160)	
$N/2++$	33.99	9.4 %	31.54	1.5 %	77.48	25.6 %	68.63	11.3 %	63.14	2.4 %
$N/2--$	33.03	6.3 %	31.28	0.7%	73.85	19.8 %	66.57	7.9 %	62.19	0.8 %
$2N/3+$	32.25	3.8 %	30.97	-0.3 %	-	-	65.1	5.6 %	61.68	0.0 %
$2N/3-$	32.12	3.4 %	30.93	-0.4 %	-	-	64.82	5.1 %	61.41	-0.4 %
$3N/4+$	31.81	2.4 %	30.93	-0.4 %	-	-	-	-	61.34	-0.5 %
$3N/4-$	31.73	2.2 %	30.92	-0.5 %	-	-	-	-	61.33	-0.5 %
$4N/5++$	31.65	1.9 %	30.09	-0.5 %	-	-	-	-	-	-
$4N/5--$	31.44	1.2 %	30.94	-0.4 %	-	-	-	-	61.44	-0.4 %
DNS	31.06				61.67					

Table 3 Mean of Nusselt numbers at the top and bottom walls, depending on the Rayleigh number, the MRF and the settings of the SVV model. For each column, the left number is the absolute value of the Nusselt number and the right one is the relative difference with the DNS value. Unstable settings are marked with symbol "-'.

4.2.3 Selection of a set of parameters Of the two parameters of the SVV model, the cut-off mode has the main influence on both the stability and the accuracy. As the MRF increases, the cut-off mode has to be reduced to ensure stability, but the accuracy of the results can be severly downgraded. Therefore, there is no configuration that allows both stability and accuracy for a high MRF. SVV modelling cannot consequently be used with a too coarse mesh and the MRF must be kept around 2.

As a compromise between stability and accuracy, the configuration $2N/3-$ was chosen in the following :

Ra	10^8				10^9					
MRF (Mesh) / Case	2.67 (60)		2 (80)		4 (80)		2.67 (120)		2 (160)	
$N/2++$	34.02	9.6 %	32.22	3.8 %	71.37	15.4 %	67.69	9.4 %	64.44	4.2 %
$N/2--$	32.44	4.5 %	31.62	1.9 %	68.03	10.0 %	66.5	7.5 %	63.08	2.0 %
$2N/3+$	32.8	5.7 %	31.58	1.7 %	-	-	66.44	7.4 %	62.95	1.7 %
$2N/3-$	32.54	4.8 %	31.48	1.4 %	-	-	65.92	6.5 %	62.57	1.1 %
$3N/4+$	31.6	1.8 %	31.26	0.7 %	-	-	-	-	61.95	0.1 %
$3N/4-$	31.74	2.3 %	31.24	0.6 %	-	-	-	-	62.07	0.3 %
$4N/5++$	33.32	7.3 %	31.15	0.4 %	-	-	-	-	-	-
$4N/5--$	32.55	4.9 %	31.15	0.4 %	-	-	-	-	62.01	0.2 %
DNS	31.04				61.87					

Table 4 Mean convective flux at the center plane of the cavity, depending of the Rayleigh number, the MRF and the settings of the SVV model. For each column, the left number is the absolute value of the convective flux and the right one is the relative gap with the DNS value. Unstable settings are marked with symbol "-'.

$M = 2N/3$, $\epsilon = 1/3N$.

5. FURTHER ANALYSIS OF THE CHOSEN SVV MODEL

5.1 Statistical analysis of the flow

Figure 3 shows the vertical distribution of key values of the flow, averaged over time and horizontal planes, obtained with DNS and with the chosen SVV model $2N/3-$, at $\mathrm{Ra} = 10^9$: temperature $\overline{\theta}$, square of temperature fluctuation $\overline{\theta'^2}$, conductive flux $-\partial\overline{\theta}/\partial x_3$, convective flux $\overline{u_3\theta}$, kinetic energy of the mean flow $\overline{u}_i\overline{u}_i/2$, and turbulent kinetic energy $\overline{u_i'u_i'}/2$. Results with the SVV model are in very good agreement with DNS. Furthermore, the LES is able to accurately predict the second-order statistics.

5.2 Autocorrelation function of the temperature field

To get an idea of the ability of SVV modelling to capture the structure of the flow, we calculated the autocorrelation function in horizontal planes of the temperature field near the bottom wall. The autocorrelation function was calculated using the Wiener-Khinchin theorem, stating that, for a stationnary random process, the Fourrier spectral decomposition of the autocorrelation function is equal to the power spectrum of this process.

Let us call $\theta_{z_0}(\boldsymbol{r})$ the two-dimensional temperature field in the plane $z = z_0$, $\widehat{\theta}_{z_0}(\boldsymbol{k})$ its Fourrier transform, and $R_{\theta_{z_0}}(\boldsymbol{r}) = \int_\Omega \theta(\boldsymbol{r'})\theta(\boldsymbol{r'}+\boldsymbol{r})d\boldsymbol{r'}$ the autocorrelation function of θ_{z_0}. Then :

$$R_{\theta_{z_0}}(\boldsymbol{r}) = \frac{1}{2\pi}\iint_{-\infty}^{\infty} ||\widehat{\theta}_{z_0}(\boldsymbol{k})||^2 \exp(2\imath\pi\boldsymbol{k}\cdot\boldsymbol{r})\, d\boldsymbol{k}. \tag{10}$$

This process is repeated for N_{fields} instantaneous temperature fields and the mean autocorrelation function of the temperature field is then defined by :

$$\overline{R_{\theta_{z_0}}}(\boldsymbol{r}) = \frac{1}{N_{\text{fields}}}\sum_{i=1}^{N_{\text{fields}}} R_{\theta_{z_0},i}(\boldsymbol{r}) \tag{11}$$

Figure 4 shows examples of instantaneous temperature fields obtained with DNS and with the SVV model $2N/3-$, at $\mathrm{Ra} = 10^9$, as well as the mean autocorrelation functions of the temperature field at z=0.007 calculated with $N_{\text{fields}} = 78$ temperature fields, with DNS and SVV simulations..

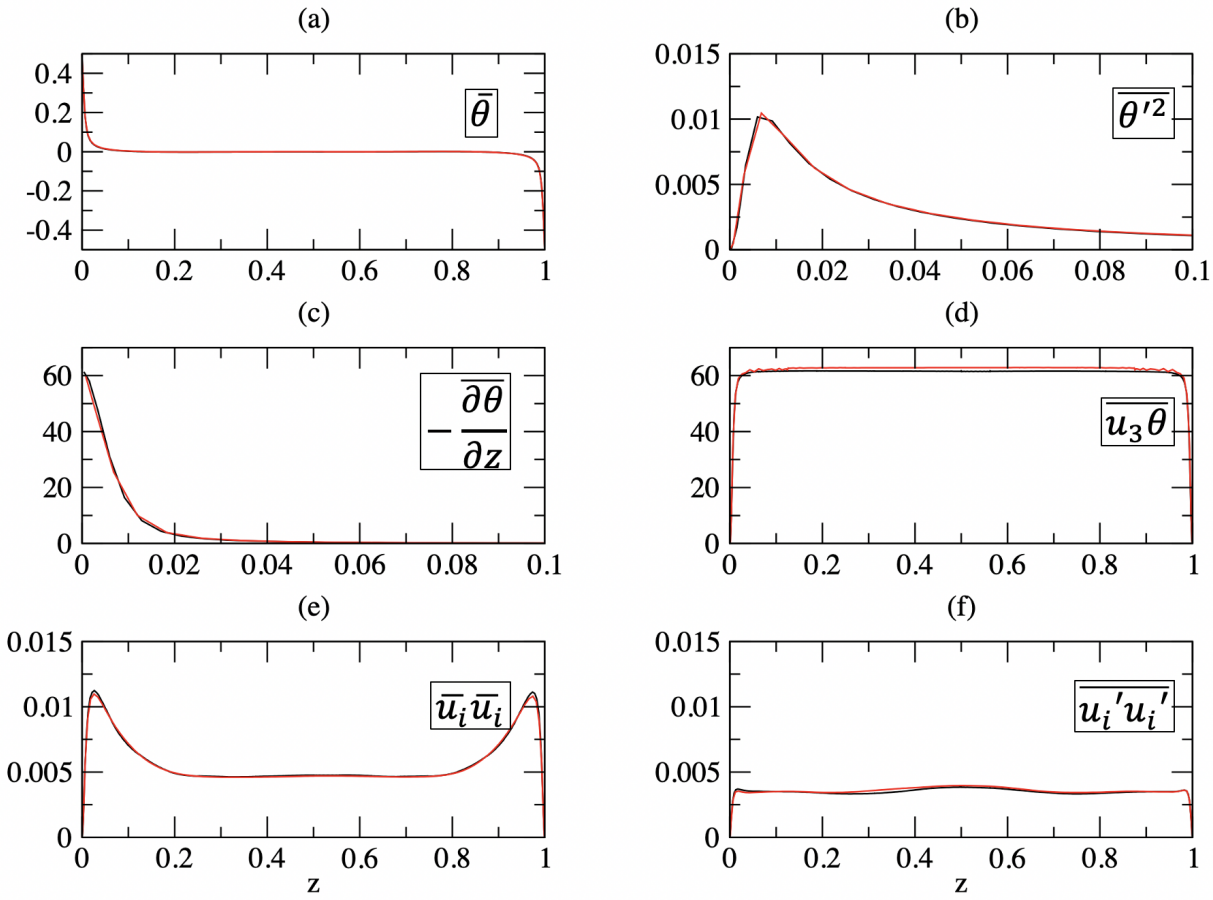

Fig. 3 Vertical distribution of key values, averaged over time and over horizontal planes, at $\mathrm{Ra} = 10^9$. (a) Temperature $\overline{\theta}$, (b) Square of temperature fluctuation $\overline{\theta'^2}$ (zoom), (c) Conductive flux $-\partial\overline{\theta}/\partial x_3$ (zoom), (d) Convective flux $\overline{u_3\theta}$, (e) Kinetic energy of the mean flow $\overline{u}_i\overline{u}_i/2$, (f) Turbulent kinetic energy $\overline{u_i'u_i'}/2$. DNS (black) and LES with the SVV model $2N/3-$ (red).

First, Figures 4 (a) and 4 (b) show similar structures with the signature of a large scale circulation organized around a diagonal plane. To further quantify these structures, the computed averaged autocorrelation functions, shown in Figures 4 (c) for DNS simulations and 4 (d) for the SVV model, are in very good agreement, indicating that the SVV model preserves the length distribution of large scale turbulent eddies and the integral scale of turbulence.

6. CONCLUSION

Spectral Vanishing Viscosity model is a very good alternative to classic eddy-viscosity models for Large Eddy Simulations and has shown many assets, since as its ability to stabilize the numerical simulations of Rayleigh-Bénard convection with Chebyshev spectral collocation method is quite robust and the numerical cost of the model is negligible. Moreover, the SVV model accurately predicts key values, such as the Nusselt number at the wall, the convective flux and the kinetic energy. It has also proven its capability of reproducing the second order statistics and preserving the large scale distribution of the turbulent eddies. It must be noted that SVV modelling does not affect the spectral convergence of the numerical method.

Of the two parameters of the SVV model, it seems that one of them has a major role in both the stability of the

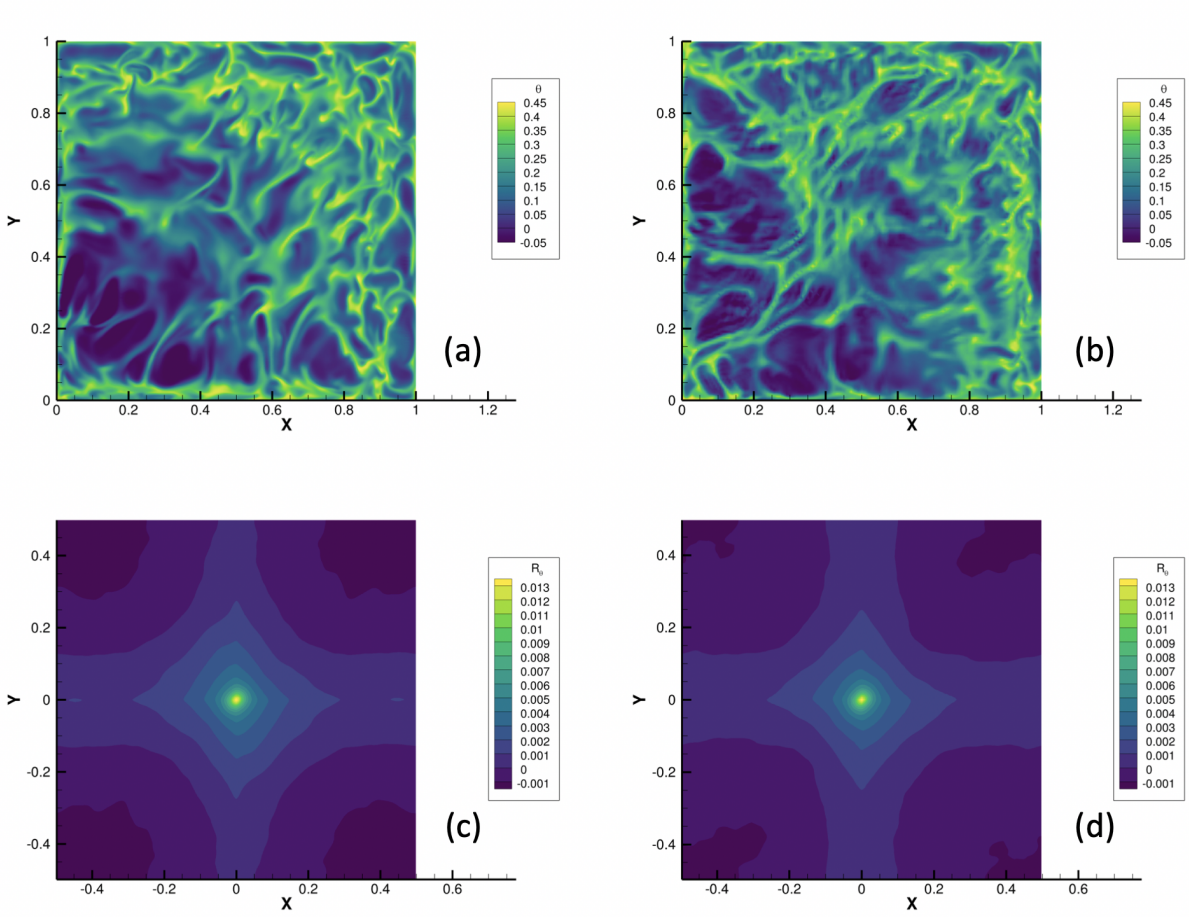

Fig. 4 Snapshots of the temperature field at z=0.007 obtained via DNS (a) and SVV, model $2N/3-$ (b). Mean autocorrelation function of the temperature field at z=0.007 for the DNS (c) and SVV (d) simulations, based on 78 snapshots. $\mathrm{Ra} = 10^9$.

simulation and the accuracy the results: the cut-off mode. The weight plays a minor role and should preferably be kept quite low. This feature leads to the the most obvious limitation of SVV simulations: the downgrade of the accuracy of the results when the reduction of the mesh gets too high. SVV model can be very accurate, but does not allow for a too coarse mesh.

ACKNOWLEDGMENTS

This work benefited from the financial support of the "Agence de l'environnement et de la maîtrise de l'énergie" (ADEME, France). This work was granted access to the HPC resources of IDRIS under the allocation 2020-A0062B00209 attributed by GENCI (Grand Equipement National de Calcul Intensif). This work was also performed using HPC resources from the Mésocentre computing center of CentraleSupélec and École Normale Supérieure Paris-Saclay supported by CNRS and Région Île-de-France (http://mesocentre.centralesupelec.fr/).

REFERENCES

[1] Andreassen, O., Lie, I., and Wasberg, C., "The Spectral Viscosity Method Applied to Simulation of Waves in a Stratified Atmosphere," *Journal of Computational Physics*, 110, pp. 257–273, (1994).

[2] Delort-Laval, M., Soucasse, L., Rivière, P., and Soufiani, A., "Rayleigh–Bénard convection in a cubic cell under the effects of gas radiation up to Ra=10^9," *International Journal of Heat and Mass Transfer*, 187, pp. 122453, (2022).

[3] J.Patterson and Imberger, J., "Unsteady natural convection in a rectangular cavity," *Journal of Fluid Mechanics*, 100, pp. 65–86, (1980).

[4] Karamanos, G. and Karniadakis, G., "A Spectral Vanishing Viscosity Method for Large Eddy Simulations," *Journal of Computational Physics*, 163, pp. 22–50, (2000).

[5] Maday, Y. and Tadmor, E., "Analysis of the Spectral Vanishing Viscosity for periodic conservation laws," *Siam Journal on Numerical Analysis*, 26, pp. 854–870, (1989).

[6] Minguez, M., Pasquetti, R., and Serre, E., "High-order large-eddy simulation of flow over the "Ahmed body" car model," *Physics of Fluids*, 20, pp. 095101, (2008).

[7] Pasquetti, R., "Spectral Vanishing Viscosity Method for Large-Eddy Simulation of Turbulent Flows," *Journal of scientific Computing*, 27, pp. 365–375, (2006).

[8] Pitz, D., Chewa, J., and Marxen, O., "Effect of an axial throughflow on buoyancy-induced flow in a rotating cavity," *International Journal of Heat and Fluid Flow*, 80, pp. 108468, (2019).

[9] Smagorinsky, J., "General circulation experiment with the primitive equations," *Monthly Weather Review*, 91, pp. 99–164, (1963).

[10] Tadmor, E., "Convergence of spectral methods for nonlinear conservation laws," *Siam Journal on Numerical Analysis*, 26, pp. 30–44, (1989).

[11] Xin, S., Chergui, J., and Le Quéré, P., "3D spectral parallel multi-domain computing for natural convection flows," , *Parallel Computational Fluid Dynamics, Lecture Notes in Computational Science and Engineering book series*Springer (Ed.), Vol. 74, pp. 163–171, (2008).

[12] Xin, S. and Le Quéré, P., "An extended chebyshev pseudo-spectral benchmark for the 8:1 differentially heated cavity," *Numerical Metholds in Fluids*, 40, pp. 981–998, (2002).